Supporting Information for:

Atomic Layer Deposition of a Sub-monolayer Catalyst for the Enhanced Photoelectrochemical Performance of Water Oxidation with Hematite

Shannon C. Riha[§,||,†], Benjamin Michael Klahr[‡,†], Eric C. Tyo[$], Sönke Seifert[x], Stefan Vajda[§,$,€], Michael J. Pellin[§,||], Thomas William Hamann[‡,*], Alex Brandon Fletcher Martinson[§,||,*]

[§]Materials Science Division, Argonne National Laboratory, Argonne, Illinois 60439, United States

[||]Argonne-Northwestern Solar Energy Research (ANSER) Center, Argonne National Laboratory, Argonne, Illinois 60439, United States

[‡]Department of Chemistry, Michigan State University, East Lansing, Michigan 48824-1322, United States

[x]X-ray Science Division, Argonne National Laboratory, 9700 South Cass Avenue, Argonne, IL 60439, United States

[$]Department of Chemical and Environmental Engineering, School of Engineering & Applied Science, Yale University, 9 Hillhouse Avenue, New Haven, CT 06520, United States

[€]Nanoscience and Technology Division, Argonne National Laboratory, 9700 South Cass Avenue, Argonne, IL 60439, United States

KEYWORDS Hematite, Fe_2O_3, photoelectrocatalysis, water oxidation, electrochemical impedance spectroscopy, X-ray absorption spectrosopy, XANES

The relative thickness of the ALD layers was determined by ellipsometry on witness Si/SiO_2 chips coated with the previous underlayer materials. For example, to get the relative thickness of the Co(II)/Co_3O_4 layer, the Si/SiO_2 chips were first coated with ITO and then Fe_2O_3. Figure S1 plots the Co(II)/Co_3O_4 thickness measured on the witness Si/SiO_2/ITO/Fe_2O_3/Co(II)-catalyst chips as a function of ALD cycle number. The growth rate estimated from this plot is ~0.6 Å/cycle, consistent with previous literature results.[1] Therefore, the estimated thickness of 1 ALD cycle Co(II)/Co_3O_4 is less than 1 Å.

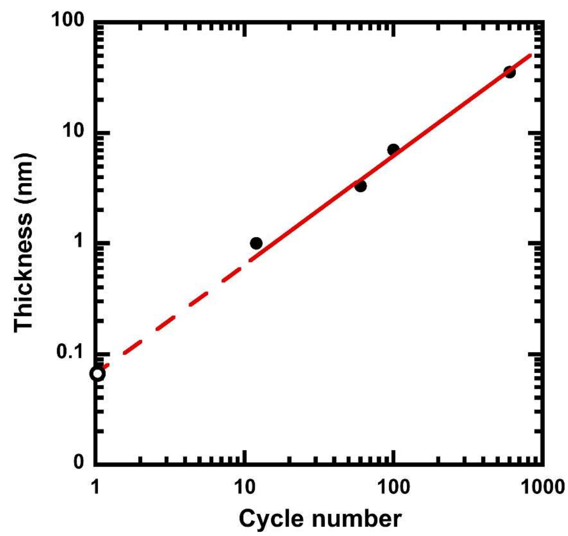

Figure S1. Co(II)/Co_3O_4 thickness as a function of ALD cycle number.

Photoelectrochemical measurements were used to analyze the effect of Co(II)/Co_3O_4 ALD-overlayers. The dark current for the bare hematite and those coated with 1 ALD cycle Co(II)/Co_3O_4 on flat substrates and inverse opal scaffolds are presented in Figure S2a. This data shows that even the dark current onsets at a more cathodic potential for the nanolaminates treated with 1 cycle Co(II)/Co_3O_4 in contrast to the bare hematite photoanodes. The J-E plots as a function of the number of Co(II)/Co_3O_4 ALD cycles are shown in Figure S2b. Three cycles of Co(II)/Co_3O_4 show some improvement over the bare hematite nanolaminate photoanode, but the cathodic shift and current enhancement is decreased in comparison to the 1 cycle of Co(II)/Co_3O_4. After 12 cycles of Co(II)/Co_3O_4, the onset potential is shifted anodically by 200 mV, however, the current steeply rises to plateau at values similar to that observed for the 1 cycle case.

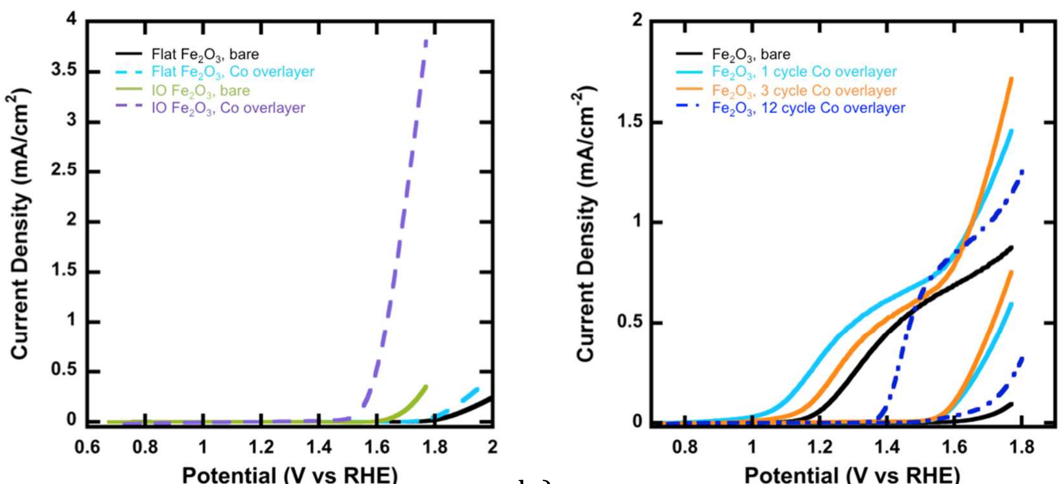

a.) b.)

Figure S2. a.) Dark current data corresponding to the photoanodes shown in Figure 2 of the main text. b.) Dark and illuminated J-E curves for the 13 nm hematite photoanodes on flat FTO-ITO substrate (black), coated with 1 (blue), 3 (orange), or 12 (dark blue dash-dot) cycles Co(II)/Co_3O_4.

Figure S3 plots the J-E stability of a flat bare hematite photoanode and one coated with 1 ALD cycle Co(II)/Co_3O_4. Between the initial J-E scan and the scan following a 3 h EIS measurement, there is a slight anodic shift observed for the sample treated with 1 ALD cycle Co(II)/Co_3O_4, while the current plateaus at the same value. There is minimal change observed for the bare hematite photoanode. After an addition 3 h constant potential measurement at an applied potential of 1.53 V vs RHE and under illumination, the J-E curve of the 1 ALD cycle Co(II)/Co_3O_4 photoanode shows little change in both the onset potential and the plateau current compared to the J-E scan taken following EIS.

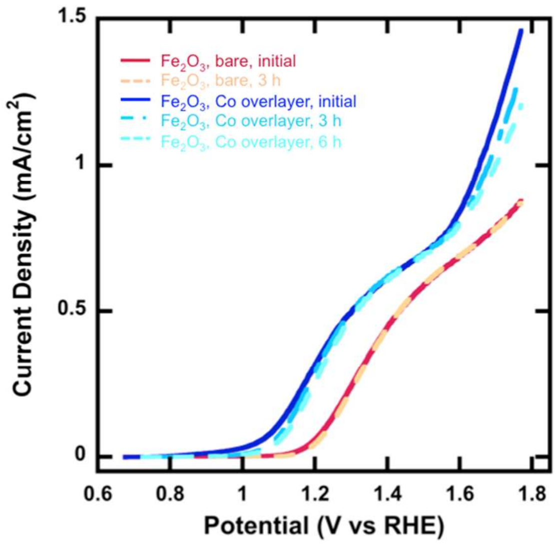

Figure S3. Initial J-E scan for bare hematite (red, solid) and with 1 ALD cycle Co(II)/Co_3O_4 catalyst (dark blue, solid). Additional J-E curves were measured for both samples after 3 h of EIS data (orange, dashed and blue, long dashed for bare and 1 cycle, respectively), and following a 3 h constant potential measurement for the 1 ALD cycle samples (6 h total, teal, short dash).

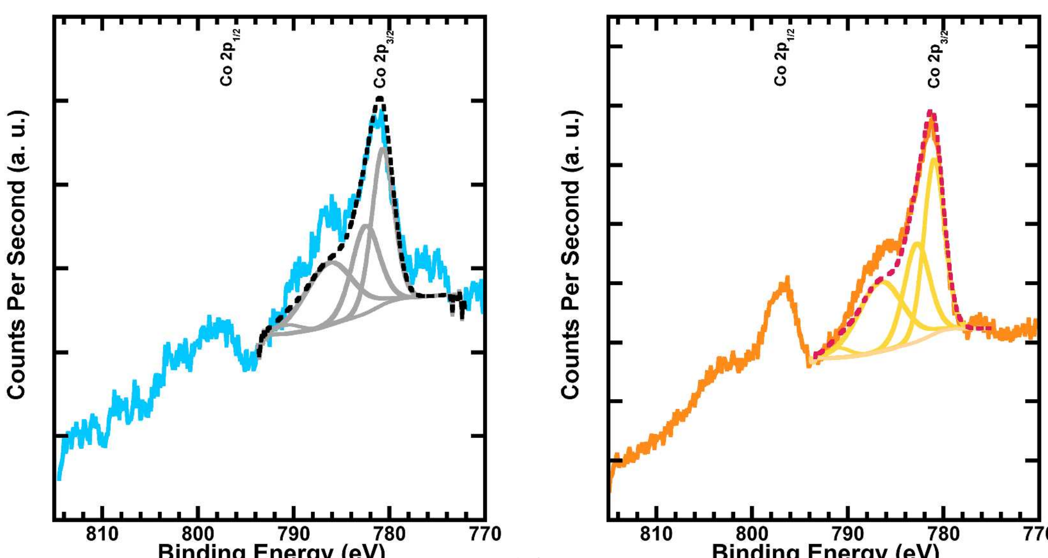

a.) b.)

Figure S4. XPS fits for a.) 1 and b.) 3 ALD cycle of Co(II)/Co_3O_4 on hematite nanolaminates. Note that the FWHM values were adjusted, but the relative ratios kept constant, to account for peak broadening in these sample.

Table S1. Co $2p_{3/2}$ spectral fitting constants: binding energy (BE, eV), spectral component separation (eV), full width at half max value (FWHM, eV), and percentage of total area (%).

	Peak1 BE (eV)	Peak1 FWHM (eV)	%	Peak2-Peak1 (eV)	Peak2 FWHM (eV)	%	Peak3-Peak2 (eV)	Peak3 FWHM (eV)	%	Peak4-Peak3 (eV)	Peak4 FWHM (eV)	%	Peak5-Peak4 (eV)	Peak5 FWHM (eV)	%
$Co(OH)_2$	780.74	2.3	38.1	1.8	2.875	26.6	3.79	5.037	33.0	4.4	2.622	2.4			
Co_3O_4	779.5	2.5	40.5	1.3	2.925	29.1	1.3	3.925	15.2	3.0	7.975	8.1	4.3	5.925	7.2

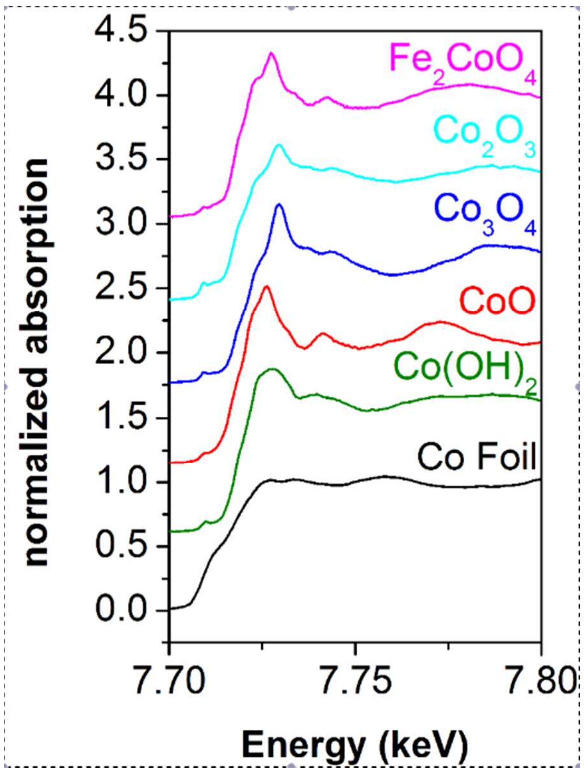

Figure S5. XANES data for various Co standards: Co foil (black), $Co(OH)_2$ (green), CoO (red), Co_3O_4 (blue), Co_2O_3 (aqua), and Fe_2CoO_4 (magenta).

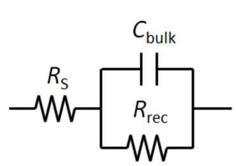

Figure S6. Randle's circuit used in the EIS data fitting.

Dopant densities were calculated from the MS plots and are 1.1 x 10^{19} and 1.6 x 10^{19} for bare and $Co(II)/Co_3O_4$-coated electrodes, respectively. The total resistance, R_{tot} was calculated ($R_s + R_{trap} + R_{ct,ss}$) and compared to the resistance derived from the J-E curve ($R_{tot} = dV/dJ$). A plot of R_{tot} derived from both impedance and J-V results can be seen in Figure S7b. The good overlap of R_{tot} derived by IS and J-E curves suggests that the assumption that charge transfer occurs through one pathway is a valid one.

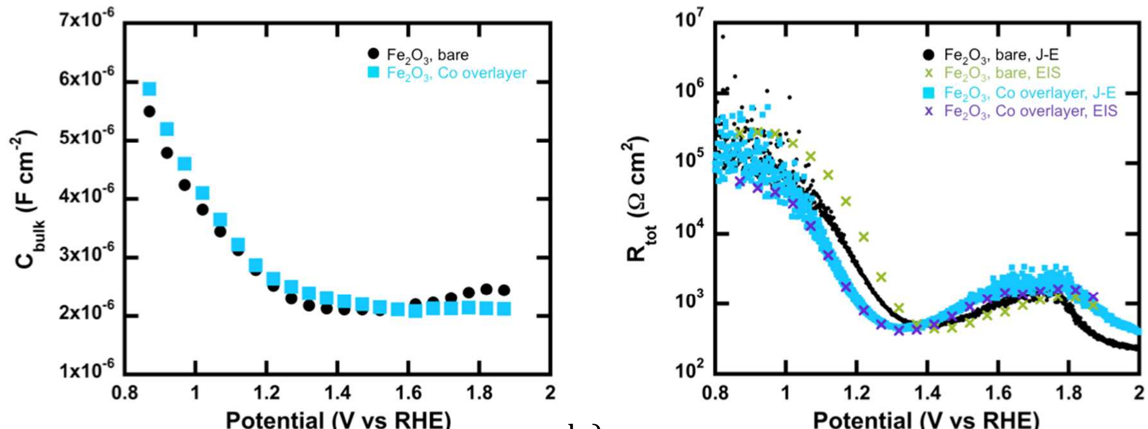

a.) b.)

Figure S7. a.) C_{bulk} determined from the EIS measurements for bare (black) hematite and with 1 ALD cycle $Co(II)/Co_3O_4$ (blue). b.) R_{tot} values calculated from EIS data and J-E curves. The green and purple × in panel c were the R_{tot} values calculated from the EIS data for bare hematite and with 1 ALD cycle $Co(II)/Co_3O_4$, respectively. The black (bare hematite) and blue traces (1ALD cycle $Co(II)/Co_3O_4$ were determined from the J-E plots).

Anodic and cathodic current transients were collected at constant potential. For anodic transients, the dark current was stabilized before exposing the photoanode to light using an automated shutter. The current was allowed to stabilize before closing the shutter, after which the cathodic current transients were recorded. No additional data manipulation was performed; however, the cathodic current transient plots have been zoomed to highlight only the transients. The amount of charge passed at each potential was determined by integrating that area of the cathodic current transient.

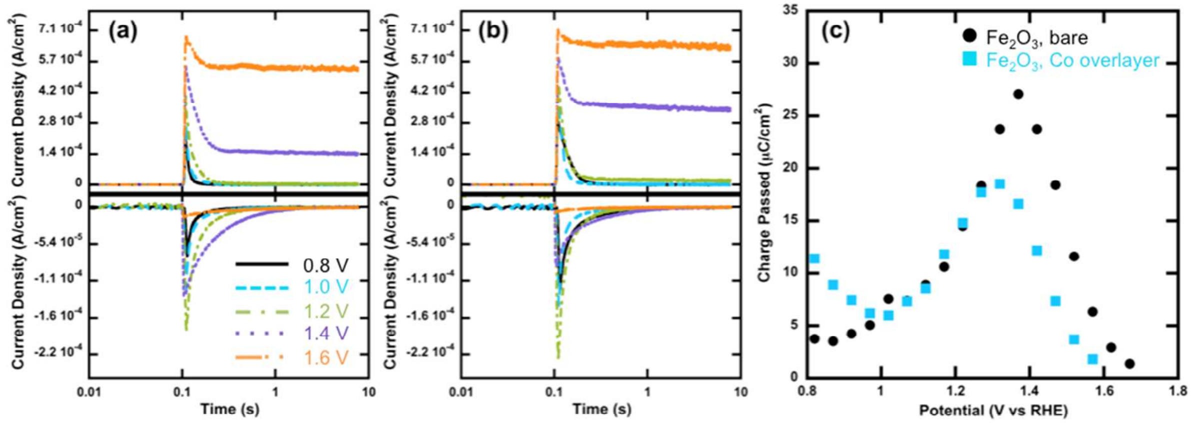

Figure S8. Anodic (top) and cathodic (bottom) transients for a.) bare hematite photoanodes and b.) with 1 ALD cycle Co(II)/Co_3O_4 at different applied potentials: 0.8 V (black, solid), 1.0 V (blue, dashed), 1.2 V (green, dash/dot), 1.4 V (purple, dotted), and 1.6 V (orange, double dash/double dot). All potentials are in reference to RHE. C.) The charge passed for bare hematite photoanodes (black circles) and with 1 ALD cycle Co(II)/Co_3O_4 (blue squares), as calculated from the area of the cathodic transients.

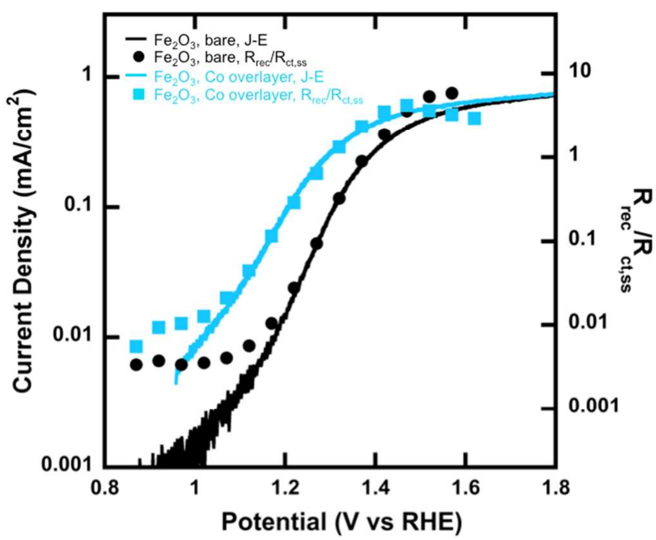

Figure S9. $R_{rec}/R_{ct,ss}$ for bare hematite photoanodes (black, circles) and hematite photoanodes with 1 ALD cycle Co(II)/Co_3O_4 (blue, squares) are overlaid on the bare and Co-modified illuminated J-E curves (black and blue traces, respectively).

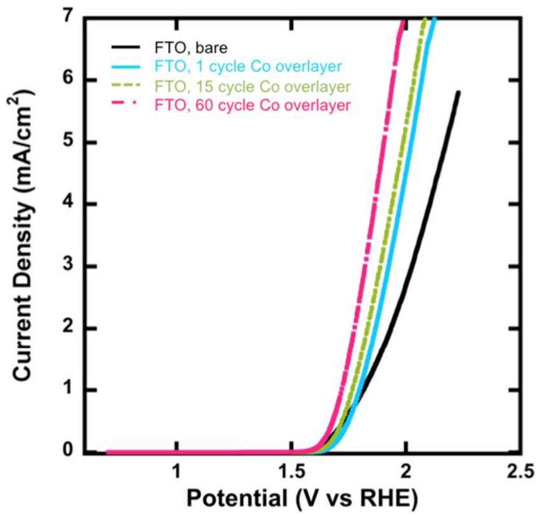

Figure S10. Dark J-E curves of bare FTO substrates coated with 1 (blue), 15 (green, dashed), or 60 (pink, dash-dot) ALD cycles Co(II)/Co_3O_4. A control FTO substrate is also plotted for comparison (black).

1. Diskus, M.; Nilsen, O.; Fjellvag, H., Thin Films of Cobalt Oxide Deposited on High Aspect Ratio Support by Atomic Layer Deposition. *Chem. Vap. Deposition* **2011,** *17*, 135-140.